



Research on the correlation between dynamic resistance and quality estimation of resistance spot welding

Dawei Zhao ^{a,b,*}, Yuriy Bezgans ^{a,*}, Yuanxun Wang ^c, Wenhao Du ^d, Nikita Vdonin ^a

^a Department of Welding Engineering, Institution of Engineering and Technology, South Ural State University, Chelyabinsk 454080, Russia

^b State Key Laboratory for Strength and Vibration of Mechanical Structures, Xi'an Jiaotong University, Xi'an 710054, China

^c Department of Mechanics, Huazhong University of Science and Technology, Wuhan 430074, China

^d Hunan Institute of Engineering, Xiangtan 411100, China

ARTICLE INFO

Keywords:

Mechanical properties
Dynamic resistance
Feature extraction

ABSTRACT

In this paper, relevant twenty features were extracted from the dynamic resistance signal of the welding operation and subsequent mathematical models incorporating the qualifying features were developed to investigate the relationship among dynamic resistance, welding quality and welding parameters based on the stepwise regression method. The results of the analysis of variance indicated the peak point location t_1 , the initial resistance value r_0 , and the first slope k_1 had little correlation with welding process parameters. The welding current is the most significant factor affecting the dynamic resistance signal, followed by welding time and electrode pressure. The welding current has significant effects on all the extracted features, while the electrode pressure only affects seven features. The model utilizing the features of r_{mean} , r_e , r_a , r_β and r_{med} was developed to predict the welding quality. r_{mean} is the most significant factor in the model whose maximum relative error is less than 10%.

1. Introduction

As one of the most frequently used welding techniques, resistance spot welding is an irreplaceable metal sheet joining process and has plenty of advantages, such as high efficiency, low cost, easy operation, and low noise. As shown in Fig. 1, during the resistance spot welding process, two electrodes press the overlapping parts of two metal plates and pass through very high welding current for a quite short period. According to Joule's law, the heat generated by the welding current melts the interfaces which form a solid joint when the welding current is shut off. Water-cooled or air-cooled electrodes are also employed to prevent the welding plates from sticking to the electrodes. Recently, resistance spot welding is widely used in such industries as automobile manufacturing, electrical equipment, rail vehicles, precision instruments, aircraft, subway, and other industries. However, in the actual production process, there exist many complex factors influencing the welding quality and the fluctuation of the welding quality usually occurs, even though the same welding process parameters are employed. Since the welding process is a highly nonlinear, multivariable coupled, and complex process with a lot of random uncertainties [1]. In this case,

it is crucial to employ suitable destructive and non-destructive tests to guarantee the welding quality and prevent the occurrence of partial failure.

Many researchers have used different kinds of destructive and non-destructive tests to assess and control the welding quality. Tensile shear tests and peel tests are the most commonly used destructive testing methods. They are usually carried out after welding. The welding joints with expulsion and undersized welds can be distinguished from one another with very high reliability [2]. These destructive testing methods, while easy to implement, are not ideal in plant production due to their low efficiency, off-line fault diagnosis and implementation cost. The nondestructive testing method, in sharp contrast to the destructive testing method, has proved to have the ability to evaluate and control the welding quality effectively utilizing quite a few process characteristics [3]. The process characteristics usually include the ultrasonic signals and some on-line signals, such as mechanical and electrical signals [4]. It is found that the features and components of these signals have very high relationships with the formation and development of the nugget in the welding process. As a result, a lot of researchers tempted to figure out these correlations and monitor the welding quality via these

* Corresponding authors at: Department of Welding Engineering, Institution of Engineering and Technology, South Ural State University, Chelyabinsk 454080, Russia (D. Zhao).

E-mail addresses: zhaodawei0322@alumni.hust.edu.cn (D. Zhao), bezgansyv@susu.ru (Y. Bezgans).

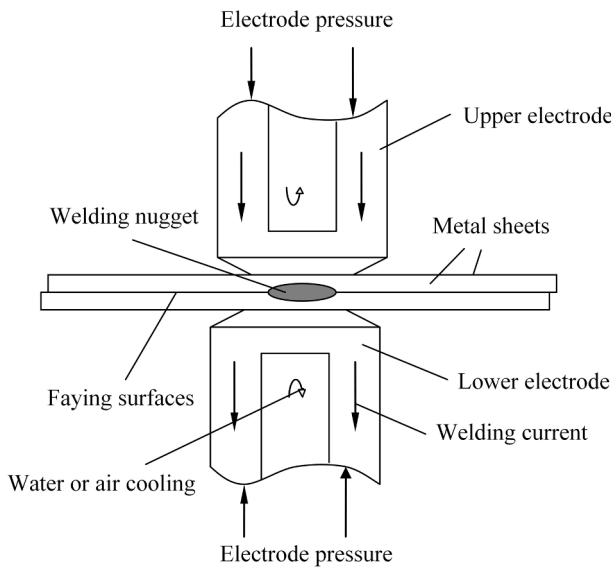


Fig. 1. A schematic diagram of the resistance spot welding process.

signals.

Among all the signals which have been studied to assess and monitor the welding quality, the dynamic resistance signal can provide the information concerning the nugget formation and development, thus it has attracted great interest of researchers in recent years. Dickinson et al. [5] pointed out that the changes of the dynamic resistance curve corresponded to the nugget formation in the welding process. According to the dynamic resistance signal, the formation and development of the welding nugget included six stages, which were the surface breakdown, asperity collapse, heating of the workpieces, molten nugget formation, nugget growth, and mechanical collapse. It was indicated that the dynamic resistance signal was very useful for monitoring and controlling the welding quality. On this basis, Gedeon et al. [6] compared the dynamic resistance curves of resistance spot welding for uncoated and galvanized steel sheets. It was found that the two dynamic resistance curves were quite different from each other. The changes in the galvanized coating during the welding process also had significant effects on the variations of the dynamic resistance signal. Its behaviors could also be clarified by the changes of dynamic resistance signal, which indicated that it was feasible and reliable to monitor the welding quality using the dynamic resistance signal. Based on the results and conclusions obtained from Dickinson et al. [5] and Gedeon et al. [6], the dynamic resistance signal is well accepted and considered as a suitable signal to monitor the welding quality.

In general, as for monitoring the welding quality, several features regarding the nugget formation and development should be extracted from the dynamic resistance curve, since a few variations of the dynamic resistance may have nothing to do with the welding quality. Besides, using a small number of characteristics rather than the complete signal to express the welding quality can simplify the calculation course, at the same time, it should also meet the accuracy requirement of engineering design and actual production conditions. In this case, features closely linked with the welding quality should be selected and isolated to demonstrate the dynamic resistance signature. Ma et al. [7] investigated the signals of dynamic resistance, electrode force and electrode tip displacement in the welding process for hot-dipped galvanized dual-phase steel DP600. It was supposed that the slope of the dynamic resistance curve between the highest peak and the bottom during the fourth and fifth periods was a proper process control strategy for monitoring the welding quality. Cho et al. [8] selected ten features from the primary circuit dynamic resistance for 0.7-mm thick uncoated low-

carbon steel sheets. The characteristics to express the dynamic resistance signal included the location of the beta peak x_1 , the rising speed after the alpha peak x_2 , the difference between the maximum and minimum values of the dynamic resistance x_3 , the maximum value of the dynamic resistance variation in each cycle x_4 , the maximum value of the dynamic resistance x_5 , the initial resistance x_6 , the final dynamic resistance x_7 , the average value of the entire dynamic resistance x_8 , the standard deviation of the dynamic resistance x_9 , and the standard deviation of the dynamic resistance variation per cycle x_{10} . Chen et al. [9] studied the dynamic resistance curve in the welding process for commercial stainless steel AISI 301 sheets with a thickness of 0.1 mm. It was indicated that the minimum resistance value could be used as a key indicator for welding nugget size and its value was inversely proportional to the nugget diameter. Karama et al. [10] investigated how to effectively monitor the welding quality for mild carbon steel sheets of 0.85 mm and grouped several dynamic resistance patterns to express the entire signal. The selected dynamic resistance patterns were treated as the inputs to establish the adaptive neuro-fuzzy inference system model, which could evaluate the welding quality with sound efficiency and validity. The extracted patterns consisted of the maximum value, the minimum value, the mean value of the resistance vector, the standard deviation value, the range value, and root mean square value of the resistance vector. Shin et al. [11] established a regression model to quantify the correlations between the extracted factors and the welding quality for 1.2 GPa ultra high strength TRIP steel. The factors were manually extracted and they included the resistance value at the alpha point x_1 , the location of the alpha point x_2 , the resistance value at the beta point x_3 , the location of the beta point x_4 , the falling speed from the initial point to the alpha point x_5 , the rising speed from the alpha point to the beta point x_6 , the mean resistance value of the entire dynamic resistance signal x_7 , the range value between the alpha point and the beta point x_8 , the value of the endpoint x_9 , and the range value between the beta point and the endpoint x_{10} . Shin et al. [12] employed a similar method and developed a regression model to estimate the welding strength for 1.2 GPa grade ultra high strength TRIP steel; the regression model had a very good performance and standard error of the estimation was about 0.1420. Xing et al. [13] utilized the random forest classification algorithm together with several manually extracted features in the dynamic resistance curve to classify all the welding joints into three categories: cold welds, good welds, and welds with expulsion. The selected patterns included the resistance value at the alpha point x_1 , the value at the beta

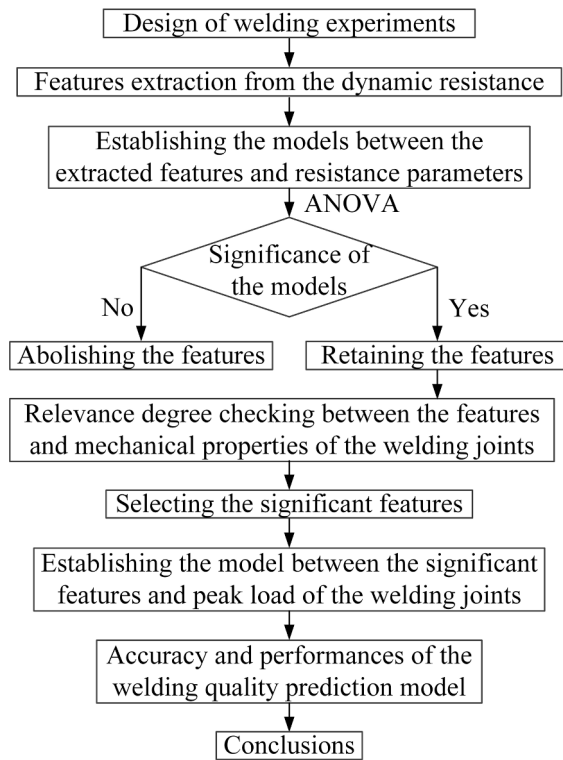


Fig. 2. The research strategy of this investigation.

point x_2 , the value at the endpoint x_3 , the relative velocity from the initial point to the alpha point x_4 , the relative velocity from the alpha point to the beta point x_5 , the relative velocity from the beta point to the endpoint x_6 , the mean resistance value x_7 , the standard deviation of the dynamic resistance signal x_8 and the maximum absolute gradient x_9 in the stage from the beta point to the endpoint. While Sun et al. [14] investigated the dynamic resistance signals with different welding qualities and it was found that the mean value of the dynamic resistance after reaching the peak point differed a lot as the welding quality varied. Wang et al. [15] also extracted some features from the dynamic resistance signal and managed to get the correlation between them and the welding strength. The results indicated that the features could be employed to monitor the welding quality. The features were manually extracted and included: the location of the beta point x_1 , the range of the resistance between the beta point and the alpha point x_2 , the rising time between the beta point and the alpha point x_3 , the resistance value at the alpha point x_4 , the declining rate between the beta point and the minimum resistance near the endpoint x_5 , the range of the resistance between the beta point and the minimum resistance near the endpoint x_6 , the mean value of the entire dynamic resistance signal x_7 , and root mean square value of the dynamic resistance signal x_8 . Zaharuddin et al. [16] extracted some features from the dynamic resistance signal and made them the inputs of the artificial neural network model to predict the welding quality of high strength steel CR780 sheets. The extracted features were beta-peak time x_1 , the rising slope between the beta point and the alpha point x_2 , the difference between the resistance values of the beta point and the endpoint x_3 , the resistance value at the beta point x_4 , the resistance value of the endpoint x_5 , the average resistance value x_6 , and the standard deviation value x_7 .

Recently, Luo et al. [17] found that the welding current and the average value of the dynamic resistance presented a linear relationship while the relationship between the welding current and the welding heat input supplied to the welding zone was quadratic polynomial. However, the relationship of other features that were usually employed by other

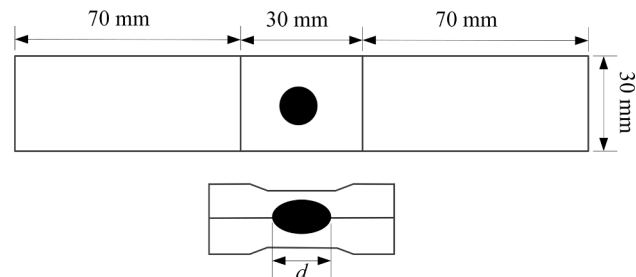


Fig. 3. The welding samples to be welded for the welding experiments (d is the nugget diameter).



Fig. 4. The schematic diagram of the welding signal acquisition system.

researchers, such as the resistance value at the endpoint [18], the value at the beta point [19] and so on, were not considered. Besides, a uniform and appropriate evaluation method for selecting the features from the dynamic resistance signal is not still available. The features are usually extracted based on experience and the results may differ significantly with different researchers. Because of the obvious subjectivity, the researchers sometimes obtained completely different conclusions. Fan et al. [20] found that the values of instantaneous drops in the dynamic resistance signal were quite valuable for monitoring the welding joints with expulsion, while Xia et al. [21] believed that no apparent relationship existed between the dynamic resistance drop and the magnitude of expulsion. In this case, it is urgent and necessary to deal with the problems of inconsistencies caused by manual extraction of the features based on experience.

Not all the variations in the dynamic resistance signal are related to the welding quality and welding process parameters. To lessen the calculative burden and improve the accuracy of the models for monitoring and evaluating the welding quality, the significant features in the dynamic resistance signal should be extracted and isolated. However, there is no theoretical basis for selecting the features. The previous research work on this issue mainly relies on observation and experience, which possesses definite subjectivity. It varies from person to person and it is difficult to eliminate the influences of contrived factors. Thus, it is necessary to establish mathematical models between the features in the dynamic resistance signal and welding process parameters to provide a basis for the selection of parameters in the dynamic resistance signal. This study is planned to resolve this issue.

In this study, a real-time monitoring system was established to obtain the welding current in the secondary circuit and voltage across the electrodes. On this basis, the dynamic resistance signal was recorded and investigated. Several features were extracted from the dynamic resistance signal, the correlation between them and welding process

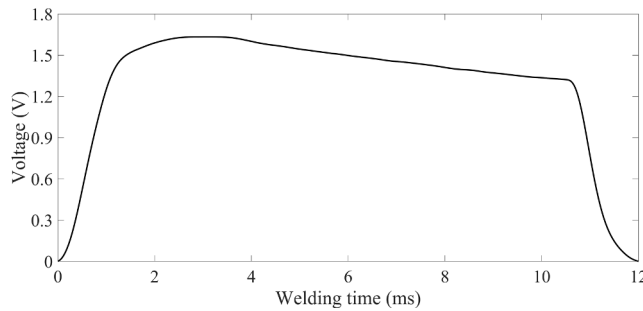


Fig. 5. The voltage curve in the welding process.

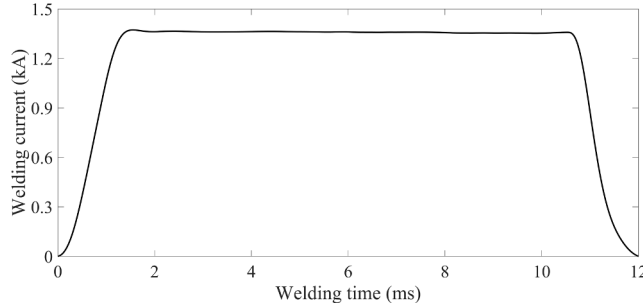


Fig. 6. The welding current in the welding process.

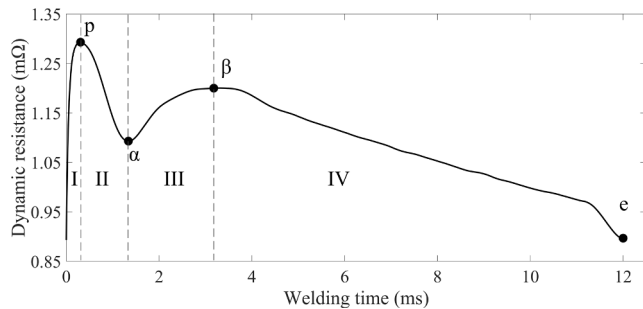


Fig. 7. The dynamic resistance signal in the welding process.

parameters were calculated. The dynamic resistance signals under different welding schedules were employed to test the validity and feasibility of the developed models. The relationships between the extracted features and the mechanical properties of the welding joints were also investigated. By analysis of variance (ANOVA), the significances of welding process parameters on the extracted features can be revealed. If one selected feature does not have a significant correlation with the changes of all the welding process parameters, it should not be included in the model for monitoring the welding quality. According to the established mathematical models and the results of ANOVA, the approach proposed in this investigation can be applied to select features in the dynamic resistance in a more accurate, objective and effective way, which can overcome the subjectivity in the previous research work. Thus, this investigation could provide a new idea and method for nondestructive testing of welding quality characteristics. Fig. 2 shows the flowchart of this investigation.

2. Materials and equipment

The material used in the welding experiments was TC2 titanium alloy with a thickness of 0.4 mm. This kind of $\alpha + \beta$ titanium alloy is welcomed owing to its advantages of lightweight, easy to be processed, and highly corrosion-resistant [22]. Its main chemical constituents (%)

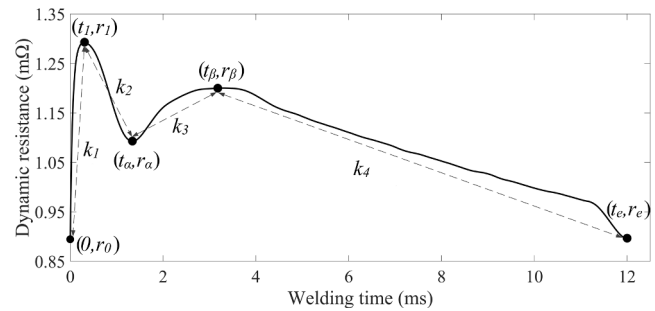


Fig. 8. Some features in the dynamic resistance signal.

are composed of Al 4.0, Mn 1.5, Fe 0.3, O 0.15, C 0.10, N 0.05, Si 0.1. The size of the samples was 100 mm \times 30 mm. The samples were welded overlay with a length of 30 mm, as shown in Fig. 3. The specimens were cleaned utilizing physical and chemical cleaning methods before welding. The mechanical properties of the welding joints were examined by the tensile shear tests. The resistance spot welding joints were carried out using a high-frequency alternating current (AC) welding machine. The model of the machine was HF-2700A high-frequency inverter spot welder produced by Miyachi Unitek. This welding machine can provide the constant current welding mode, constant voltage welding mode, and constant power welding mode. The constant current mode was employed in this study. The electrodes were made of copper alloy and the diameter of the electrode tip was 3 mm.

The dynamic resistance signal was recorded in the welding process; the measurement system was presented in Fig. 4. The voltage across the electrodes $U(t)$, as well as the welding current $I(t)$, was tested in real-time. A Rogowski coil was used to measure the welding current, while the electrode was obtained via a simple alligator clip cable. A signal conditioner produced by Miyachi Unitek was used to process the signals which were detected in the welding process, while the computer together with the acquisition unit was employed to further process and analyze the signals.

3. Results and discussion

3.1. Properties of dynamic resistance signals

The signals of the voltage $U(t)$ and welding current $I(t)$ were obtained and shown in Fig. 5 and Fig. 6. The corresponding welding current is 1.4 kA, the welding time is 12 ms and the electrode pressure is 7 MPa. The high-frequency AC welding current was employed by the resistance spot welding machine, whose operating frequency ensures that the fluctuation in the current and voltage signal is very tiny and can be ignored. In this case, the dynamic resistance signal $R(t)$ during the welding periods can be easily obtained according to the following formula,

$$R(t) = U(t)/I(t) \quad (1)$$

where t is the welding time.

Fig. 7 shows a typical resistance signal in the welding process. According to the variations of the signal, four stages can be divided into the dynamic resistance curve. The resistance increases at the beginning of the welding process until it reaches its maximum peak value. This value is considered to be related to the levels and types of welding current. During this stage, the welding current is not stable and very small (Fig. 6), the welding heat generated by the welding current is quite limited. It is generally believed that this stage has little information on the welding nugget [23]. The presence of this stage is owing to the high-frequency AC welding current employed in the welding experiments. As for industrial frequency AC, the resistance value was calculated by the

Table 1

The description of the extracted features in the dynamic resistance signal.

Features	Equation	Unit	Description
r_{mean}	$r_{mean} = \sum_i^n r_i / n$	mΩ	The average value of the whole dynamic resistance signal
σ	$\sigma = \sqrt{\frac{1}{n} \sum_{i=1}^n (r_i - r_{mean})^2}$	mΩ	The standard deviation value of the dynamic resistance signal
Δ	$\Delta = r_{max} - r_{min}$	mΩ	The range value between the maximum point and the minimum point in the dynamic resistance signal
r_e	–	mΩ	The resistance value at the endpoint
P	$P = \int r(t) dt$	mΩ-ms	Numerical integration value of the dynamic resistance curve in the welding process
r_{max}	–	mΩ	The maximum resistance value of the entire dynamic resistance signal
r_{min}	–	mΩ	The minimum resistance value of the entire dynamic resistance signal
r_{mid}	$r_{mid} = \frac{r_{max} + r_{min}}{2}$	mΩ	The average value of the maximum resistance and minimum resistance value
r_{med}	–	mΩ	The median resistance value of the entire dynamic resistance signal
r_0	–	mΩ	The resistance value at the initial point
t_1	–	ms	The location of the peak point
r_1	–	mΩ	The resistance value at the first peak point
t_a	–	ms	The location of the alpha point
r_a	–	mΩ	The resistance value at the alpha point
t_β	–	ms	The location of the beta point
r_β	–	mΩ	The resistance value at the beta point
k_1	$k_1 = \frac{r_1 - r_0}{t_1}$	Ω/s	The increasing rate between the peak point and the initial point
k_2	$k_2 = \frac{r_1 - r_a}{t_a - t_1}$	Ω/s	The decreasing rate between the peak point and the alpha point
k_3	$k_3 = \frac{r_\beta - r_a}{t_\beta - t_a}$	Ω/s	The increasing rate between the alpha point and the beta point
k_4	$k_4 = \frac{r_\beta - r_e}{t_e - t_\beta}$	Ω/s	The decreasing rate between the beta point and the endpoint

peak value of the welding current and voltage within each half cycle, it is very difficult to obtain the dynamic resistance value at this stage since the peak values are very tiny [24]. As the welding current goes up and becomes stable, the generated heat owing to the contact resistance accumulates, which makes the welding plates softened. Under this circumstance, the contact areas increase with the assistance of the electrode pressure, the dynamic resistance decreases until it gets to the alpha point. After the metal plates are in intimate contact, the temperature of the welding zone increases; the resistivity of the titanium alloy also increases with the temperature [25]. In this case, the dynamic resistance goes up in this stage. The metal begins to melt once the temperature is high enough and gets to its melting point; the dynamic resistance rises until it reaches the beta point. This point indicates that the metal has melted and propagated to a certain extent [17]. In the fourth stage, the welding nugget has attained to a certain volume; the heat dissipated by the nugget and the electrodes exceeds over the heat generated by the welding current, the dynamic resistance declines and

then reaches its endpoint. Based on the variations of the dynamic resistance signal, some features were extracted from the dynamic resistance curve. Some of the features are shown in Fig. 8. Due to the high-frequency AC welding current, the resistance value at the peak point was chosen. The locations of the alpha and beta points and the resistance values of these two points were also extracted. According to Wen's research work [18], the resistance at the endpoint was highly related to the nugget size, in this case, it was also selected in this work. Luo et al. [17] found that the mean value of the entire dynamic resistance signal and the numerical integration of the dynamic resistance curve could be employed to represent the welding quality, and they were also extracted. In addition, some statistical characteristics including the standard deviation and range of the whole dynamic resistance signal were extracted; the slopes between the five important points (initial point, peak point, alpha point, beta point, and endpoint) of the dynamic resistance were also calculated, as shown in Table 1.

The welding experiments were arranged based on the two-level factorial experimental design; the electrode pressure (EP), welding current (WC) and welding time (WT) were chosen as the welding process parameters. The welding current changed from 1.2 kA to 2.4 kA, the range of the welding time was 8 ms to 12 ms, while the electrode pressure increased from 6 MPa to 8 MPa. The twenty features were extracted from the dynamic resistance signal and treated as the outputs. The results are shown in Table 2.

3.2. Establishing models for the extracted features

As one of the most frequently used statistical and mathematical techniques, the regression analysis is often employed to quantify the relationship between the independent variables and the responses. The least-square method is usually employed to establish the regression model, while ANOVA is carried out to judge the significance of the model and its corresponding items.

The independent variables (x_1, x_2, \dots, x_n) are usually obtained based on the experimental work and they are continuous; the accuracy of the results can be guaranteed. The functional relationship quantifying the response of interest and the independent variables x_1, x_2, \dots, x_n can be calculated as follows [26]:

$$y = f(x_1, x_2, \dots, x_n) \quad (2)$$

The quadratic polynomial function is usually employed to approximately express the formula (2), which can be expressed as follows,

$$f(x_1, x_2, \dots, x_n) = a_0 + \sum_{i=1}^n a_i x_i + \sum_{i=1, j=1}^n a_{ij} x_i x_j + \varepsilon \quad (3)$$

Where ε is the error of this quadratic polynomial model, variables x_1, x_2, \dots, x_n are the independent variables, $f(x_1, x_2, \dots, x_n)$ denotes the dependent variable, the regression coefficients a_0, a_i, a_{ij} are obtained using the least-square regression method. The results of ANOVA of the mathematical model for the mean resistance r_{mean} and welding process parameters are tabulated in Table 3.

Regarding this investigation, $f(x_1, x_2, \dots, x_n)$ is the model for the welding process parameters and the extracted features in the dynamic resistance signal. The stepwise regression method and the least-square method were performed via the software Design Expert. The significance of every term in the quadratic polynomial model was evaluated by its corresponding P-value (95% confidence level) [27] and the P-value should be smaller than 0.1 [28]. The term whose P-value is smaller than 0.05 is very significant. In this case, the term EP is not significant as its P-value is above 0.1. The mean value is very sensitive to the changes of WC, WT, EP × WC, EP × WT and WC × WT. WC is the most important factor influencing the average resistance value, followed by WT. The factor EP affects this feature by the interaction effects with WC and WT. The fitting degree can be distinguished according to the coefficient of determination R^2 , the adjusted R^2 , and prediction error sum of squares.

Table 2

The results of the welding experiments.

EP	WC	WT	r_{mean}	σ	Δ	r_e	P	r_{max}	r_{min}	r_{mid}	r_{med}	t_1
6	1.2	8	1.496	0.548	2.445	1.121	11.968	3.563	1.119	2.341	1.358	0.235
8	1.2	8	1.479	0.472	2.322	1.201	11.836	3.322	1.000	2.161	1.351	0.207
6	2.4	8	0.777	0.211	0.874	0.516	6.215	1.389	0.516	0.952	0.713	0.291
6	1.2	12	1.310	0.246	1.555	1.057	15.719	2.373	0.818	1.596	1.266	0.251
8	2.4	12	0.813	0.169	0.852	0.568	9.752	1.352	0.500	0.926	0.771	0.263
8	2.4	8	0.856	0.191	0.824	0.610	6.847	1.433	0.610	1.021	0.808	0.263
6	2.4	12	0.834	0.287	1.598	0.540	10.012	2.048	0.450	1.249	0.749	0.199
8	1.2	12	1.210	0.175	0.920	1.018	14.516	1.926	1.006	1.466	1.185	0.259
EP	WC	WT	r_1	t_a	r_a	t_β	r_β	r_0	k_1	k_2	k_3	k_4
6	1.2	8	3.563	1.581	1.359	2.978	1.387	2.500	4.521	1.638	0.020	0.053
8	1.2	8	3.322	1.581	1.350	2.814	1.377	1.000	11.239	1.435	0.022	0.034
6	2.4	8	1.389	1.352	0.928	1.495	0.928	0.646	2.556	0.435	0.004	0.063
6	1.2	12	2.373	1.514	1.241	3.840	1.368	0.818	6.192	0.896	0.055	0.038
8	2.4	12	1.352	1.323	0.977	1.871	0.997	0.500	3.237	0.354	0.036	0.042
8	2.4	8	1.432	1.147	0.993	1.565	1.014	0.659	2.940	0.497	0.050	0.063
6	2.4	12	2.048	1.465	1.015	1.672	1.016	0.450	8.022	0.816	0.005	0.046
8	1.2	12	1.926	1.449	1.159	3.298	1.263	1.064	3.331	0.644	0.056	0.028

Low prediction error sum of squares and a large R^2 imply that this model is good and satisfying. The coefficient of determination R^2 is 0.9999 for the mean resistance r_{mean} implying that nearly all the experimental data confirm the compatibility with the data predicted by the model. The Pred R^2 and adjusted R^2 are quite close to the determination R^2 . The

term Adeq Precision is the measurement of the signal to noise ratio. Its value is 124.2938, which is much greater than 4. All in all, the results indicate that the developed model is good enough to navigate the design space. The regression coefficients for the model were calculated and presented as follows,

$$r_{mean} = 2.7938 + 0.0418 \times EP - 1.2065 \times WC - 0.03554 \times WT + 0.03638 \times EP \times WC - 0.01148 \times EP \\ \times WT + 0.04902 \times WC \times WT \quad (4)$$

Table 3The results of ANOVA for the mean resistance r_{mean} .

Source	Sum of squares	df	Mean square	F-value	P-value
Model	0.6743	6	0.1124	2969.5650	0.0140
EP	0.0005	1	0.0005	11.8906	0.1797
WC	0.6137	1	0.6137	16216.71	0.0050
WT	0.0244	1	0.0244	645.2768	0.0250
EP × WC	0.0038	1	0.0038	100.6908	0.0632
EP × WT	0.0042	1	0.0042	111.3389	0.0602
WC × WT	0.0277	1	0.0277	731.4849	0.0235
Residual	0.0000378	1	0.0000378		
Cor Total	0.674337	7			

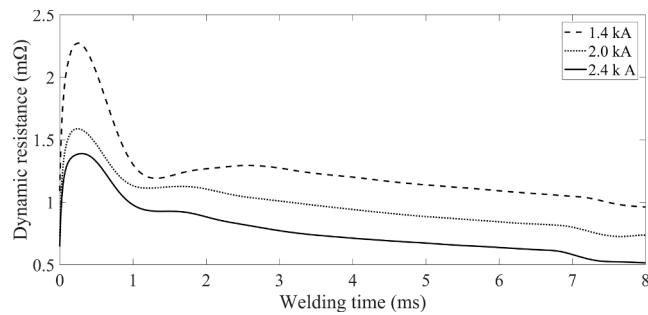
Notes: standard deviation = 0.006152, mean = 1.0967, R^2 = 0.9999, Adj R^2 = 0.9996, Pred R^2 = 0.9964, predicted residual error sum of squares (PRESS) = 0.002422, coefficient of variation (C. V.) % = 0.5609, Adeq precision = 124.2938.

Subjected to

$$\begin{aligned} & 1.2 \text{ kA} \leq WC \leq 2.4 \text{ kA} \\ & 8 \text{ ms} \leq WT \leq 12 \text{ ms} \\ & 6 \text{ MPa} \leq EP \leq 8 \text{ MPa} \end{aligned} \quad (5)$$

WC is the welding current, WT is the welding time, while the EP is the electrode pressure. It can be seen that the average resistance value decreases with the increasing welding current. The adjusted R^2 is up to 0.9996, the relationship between the welding current and the average resistance is almost in an inverse proportion, which is the same as Luo's research work [19]. It can also be concluded that the mean value of the dynamic resistance can be used as an index to monitor the welding quality.

The regression analysis was also employed to quantify the relationships between the welding process parameters and other extracted features. The ANOVA results of the regression models for the welding

**Fig. 9.** The dynamic resistance signals with different welding currents (welding time of 8 ms, electrode pressure of 6 MPa).

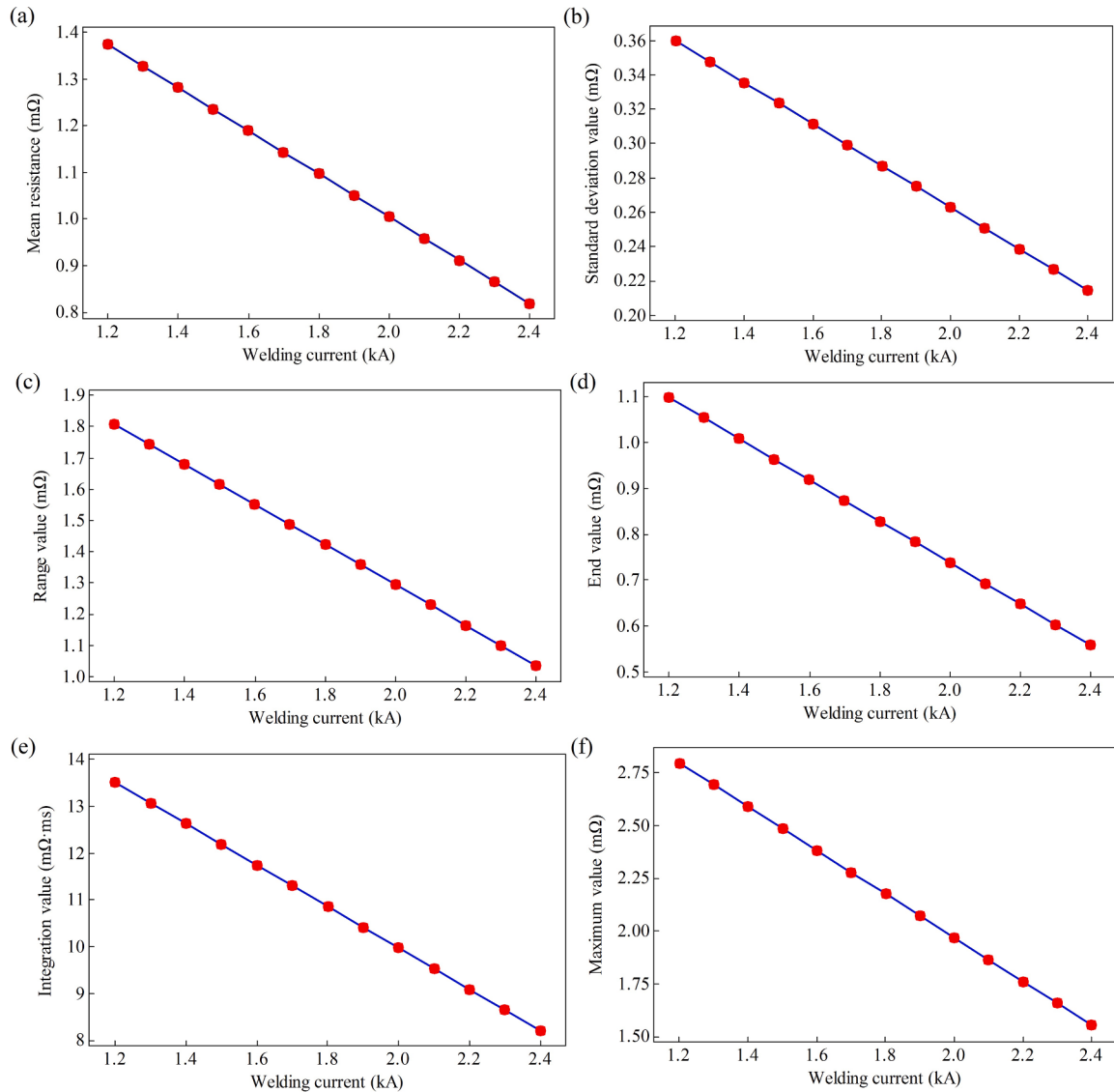


Fig. 10. The effects of the welding currents on the mean resistance r_{mean} (a), the standard deviation σ (b), the range Δ (c), the end value r_e (d), integral value P (e), and the maximum value r_{max} (f).

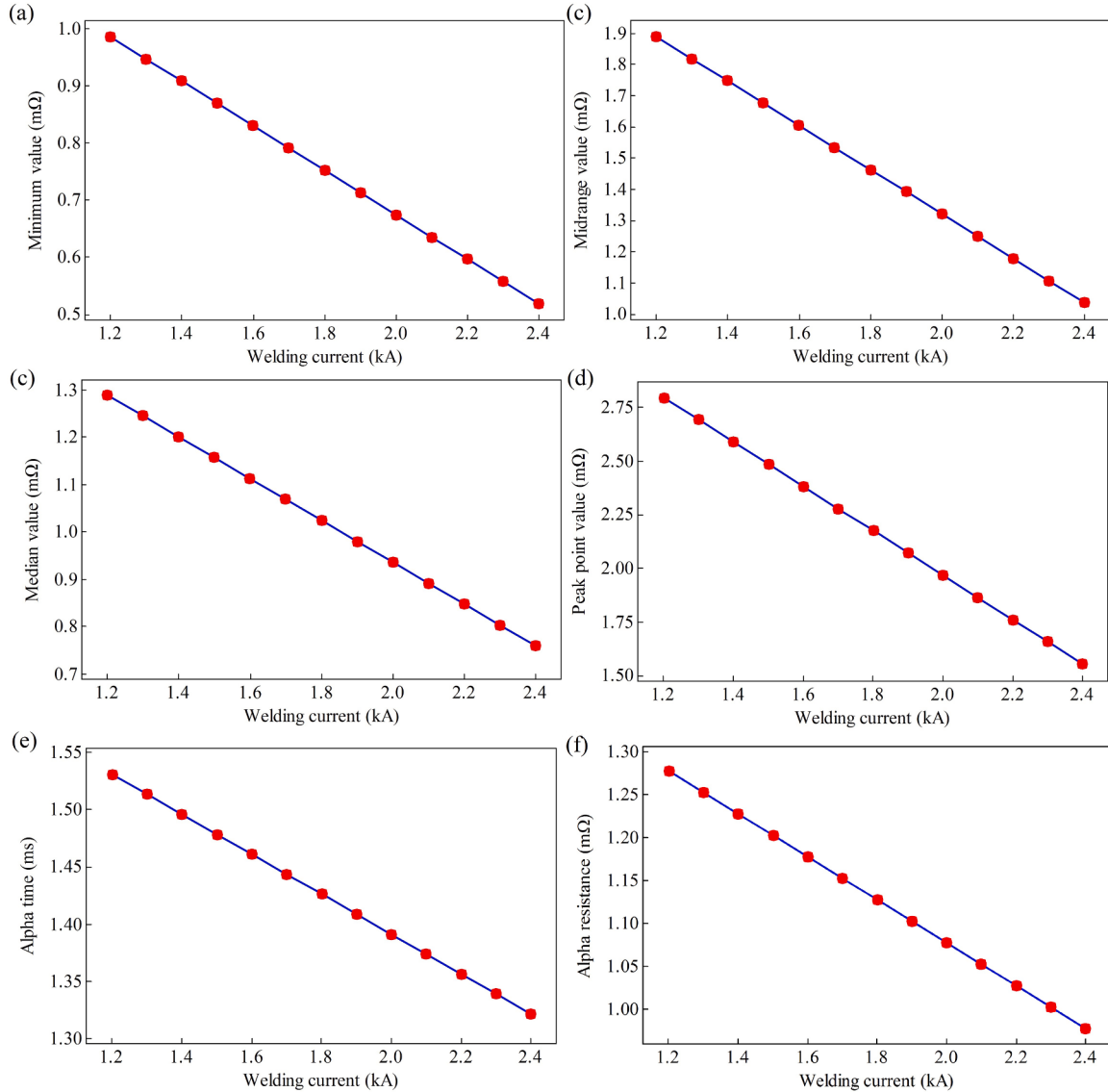


Fig. 11. The effects of the welding currents on the minimum resistance r_{min} (a), the midrange value r_{mid} (b), the median value r_{med} (c), the peak resistance r_1 (d), the alpha time t_α (e), the alpha resistance r_α (f).

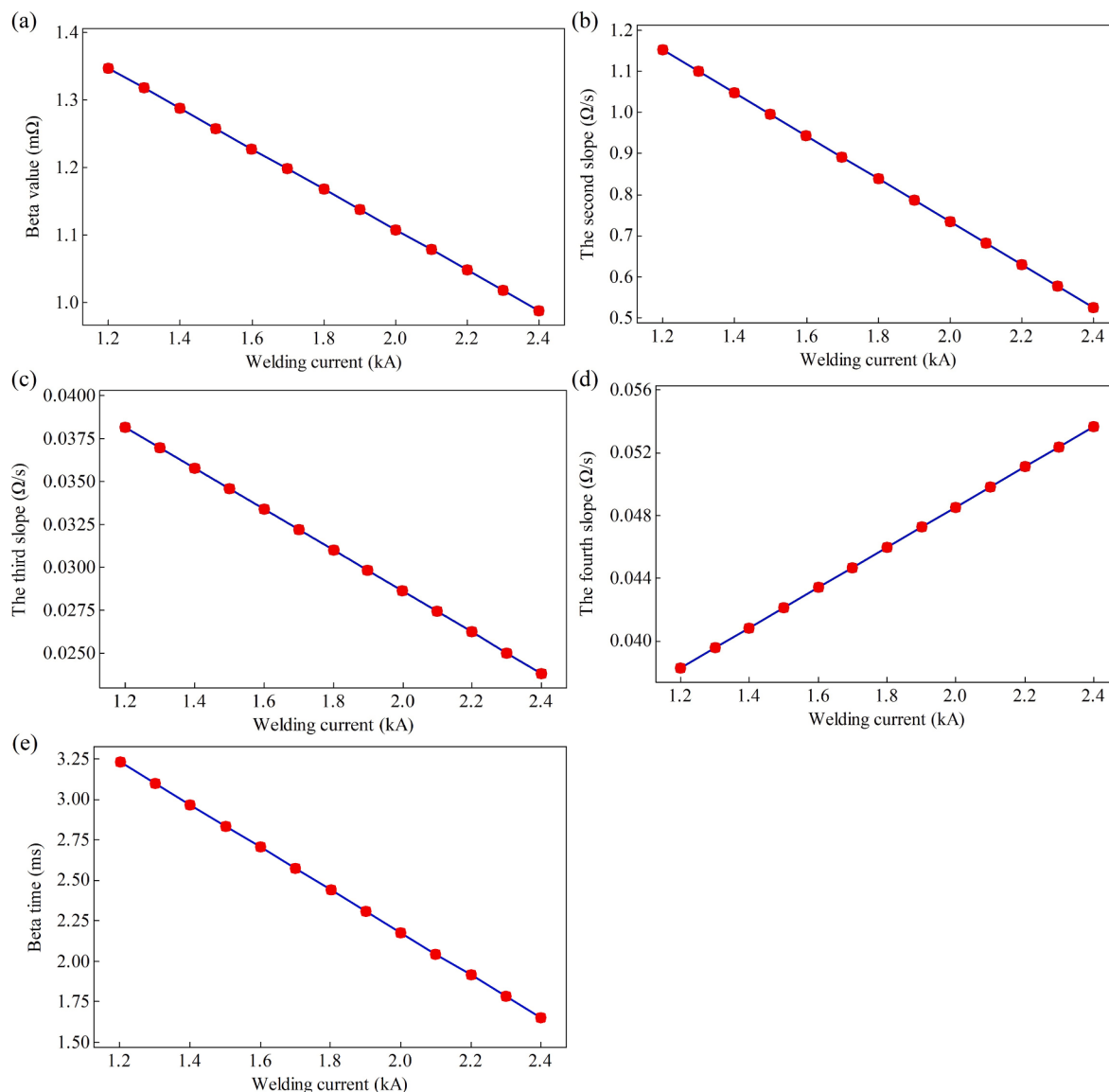


Fig. 12. The effects of the welding currents on the beta resistance r_β (a), the second slope k_2 (b), the third slope k_3 (c), the fourth slope k_4 (d) and beta time t_β (e).

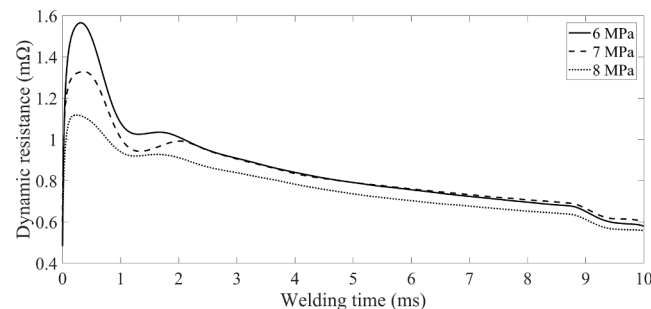


Fig. 13. The dynamic resistance signals with different electrode pressures (welding current of 2.2 kA, welding time of 10 ms).

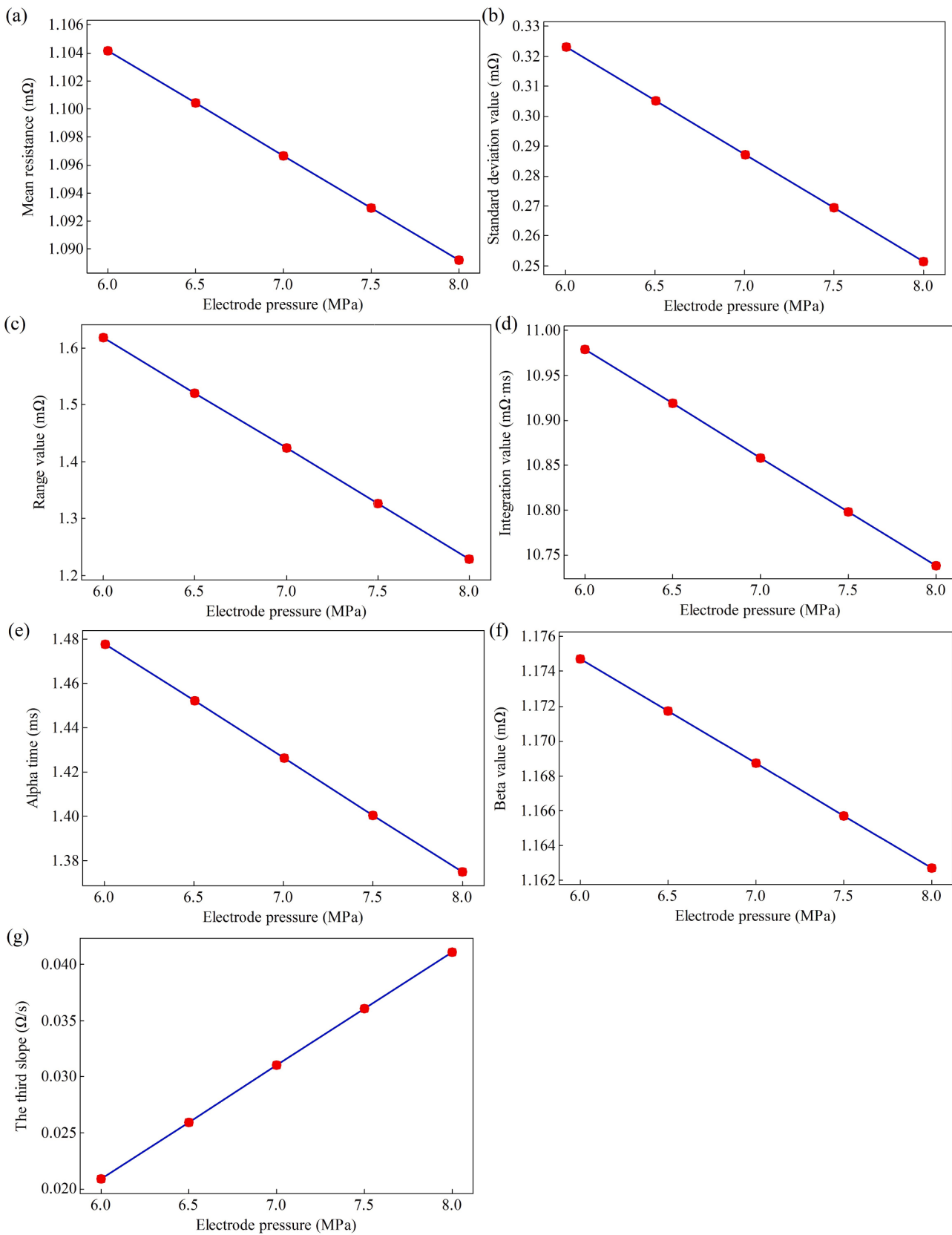


Fig. 14. The effects of the electrode pressures on the mean resistance r_{mean} (a), the standard deviation σ (b), the range Δ (c), the integral value P (d), the alpha time t_α (e), the beta resistance r_β (f) and the third slope k_3 (g).

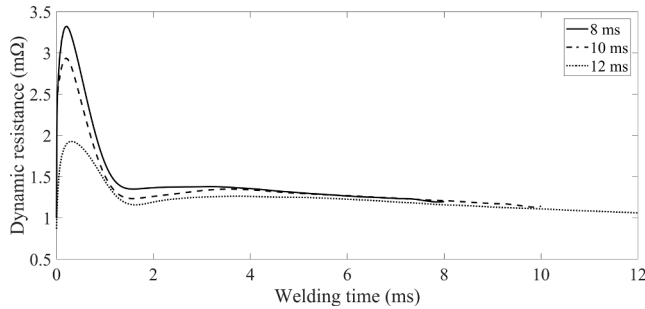


Fig. 15. The dynamic resistance signals with different welding times (electrode pressure of 8 MPa, welding current of 1.2 kA).

process parameters and the extracted features are shown in Tables 4-22 (in Appendix). It can be seen that the features t_1 , r_0 and k_1 are not sensitive to the changes of the process parameters, so these features should not be used to monitor the welding quality. The developed models for quantifying the welding process parameters and other extracted features are listed as follows,

$$\begin{aligned} \sigma = & 2.3192 - 0.03578 \times EP - 0.8008 \times WC - 0.1563 \times WT + 0.06796 \\ & \times WC \times WT \end{aligned} \quad (6)$$

$$\Delta = 5.3269 + 0.5610 \times EP - 3.8158 \times WC - 0.1383 \times WT - 0.07552 \times EP \times WT + 0.3171 \times WC \times WT \quad (7)$$

$$r_e = 1.6404 - 0.4510 \times WC \quad (8)$$

$$\begin{aligned} P = & 7.3401 + 0.4664 \times EP - 6.9101 \times WC + 1.6799 \times WT + 0.3558 \times EP \\ & \times WC - 0.1227 \times EP \times WT \end{aligned} \quad (9)$$

$$r_{max} = 11.2231 - 4.3291 \times WC - 0.7187 \times WT + 0.3295 \times WC \times WT \quad (10)$$

$$r_{min} = 1.7459 - 0.3892 \times WC - 0.02932 \times WT \quad (11)$$

$$r_{mid} = 6.5962 - 2.4212 \times WC - 0.3852 \times WT + 0.1710 \times WC \times WT \quad (12)$$

$$r_{med} = 1.82 - 0.4417 \times WC \quad (13)$$

$$r_1 = 11.2255 - 4.3308 \times WC - 0.7189 \times WT + 0.3297 \times WC \times WT \quad (14)$$

$$\begin{aligned} t_a = & 2.2198 + 0.05425 \times EP - 0.2717 \times WC - 0.08588 \times WT - 0.05875 \\ & \times EP \times WC + 0.05083 \times WC \times WT \end{aligned} \quad (15)$$

$$r_\alpha = 2.4386 - 0.6459 \times WC - 0.08623 \times WT + 0.03968 \times WC \times WT \quad (16)$$

$$t_\beta = 3.6711 - 1.3181 \times WC + 0.1143 \times WT \quad (17)$$

$$\begin{aligned} r_\beta = & 1.7750 - 0.05068 \times EP - 0.7774 \times WC + 0.04531 \times WT + 0.03788 \\ & \times EP \times WC - 0.01249 \times EP \times WT + 0.02123 \times WC \times WT \end{aligned} \quad (18)$$

$$k_2 = 5.9079 - 2.367 \times WC - 0.4127 \times WT + 0.1843 \times WC \times WT \quad (19)$$

$$\begin{aligned} k_3 = & -0.01391 - 0.0176 \times EP - 0.03346 \times WC + 0.01896 \times WT + 0.01540 \\ & \times EP \times WC - 0.00863 \times WC \times WT \end{aligned} \quad (20)$$

$$k_4 = 0.05944 + 0.01284 \times WC - 0.00365 \times WT \quad (21)$$

Where

$$\begin{aligned} 1.2 \text{ kA} \leq WC \leq 2.4 \text{ kA} \\ 8 \text{ ms} \leq WT \leq 12 \text{ ms} \\ 6 \text{ MPa} \leq EP \leq 8 \text{ MPa} \end{aligned} \quad (22)$$

From all the established models, it can be concluded that all the extracted features are influenced by the welding current. The welding current is the most significant factor for all the extracted factors except for σ and k_3 according to its P-value. The electrode pressure is only quite related to only seven extracted features and it is the least significant parameter among the three welding parameters (welding current, welding time and electrode pressure) except for the features Δ and k_3 . The features r_e and r_{med} are only influenced by the welding current. Although the interactions of the welding parameters had non-negligible effects on the features, one single feature is not able to represent the welding quality of the welding joints. In this case, the interaction effects will not be discussed in this investigation.

3.3. Verification of the regression models

Fig. 9 shows the dynamic resistance signals with different welding currents. Fig. 10, Fig. 11, and Fig. 12 exhibit the effects of the welding currents on the extracted features from the dynamic resistance signals based on the regression models (4)-(22). The peak point, alpha point, beta point, and endpoint decline with the increase of the welding current, while their corresponding times arrive in advance. Under the low current conditions, the heating rate is relatively slow; therefore, more time is required to achieve similar nugget growth and melt the metal plates. Since the welding heat is proportional to the square of the welding current, higher welding currents indicate that the shorter time is required to achieve the same amount of welding heat and nugget formation. According to the developed models (4)-(22), the end value r_e and median resistance r_{med} are only influenced by the welding current, and their values of the determination R^2 are respectively 0.9605 and 0.9578. Thus, it can be concluded that these two features can be used to represent the welding current to monitor and predict the welding quality. Wen et al. [18] employed the endpoint value of the dynamic resistance curve and other parameters as the inputs for the estimation system of welding quality; the accuracy of this system was 5.6%. Besides, the statistical characteristics of standard deviation σ , range Δ , the maximum resistance r_{max} , the minimum resistance r_{min} , the midrange value r_{mid} and the median value r_{med} decrease as the welding current goes up. This phenomenon is very easy to be revealed by Fig. 9. The rate k_4 of the decreasing stage from the beta point and the endpoint increases with the welding current [15], it is believed that this feature is highly related to the welding nugget size, higher welding current indicates a larger welding nugget size [13], and thus the declining rate is increasing. If the extremely high welding current is used, the expulsion tends to occur. During the expulsion, the dynamic resistance at this stage experiences a sudden drop [20], in this case, the feature k_4 should be pretty high.

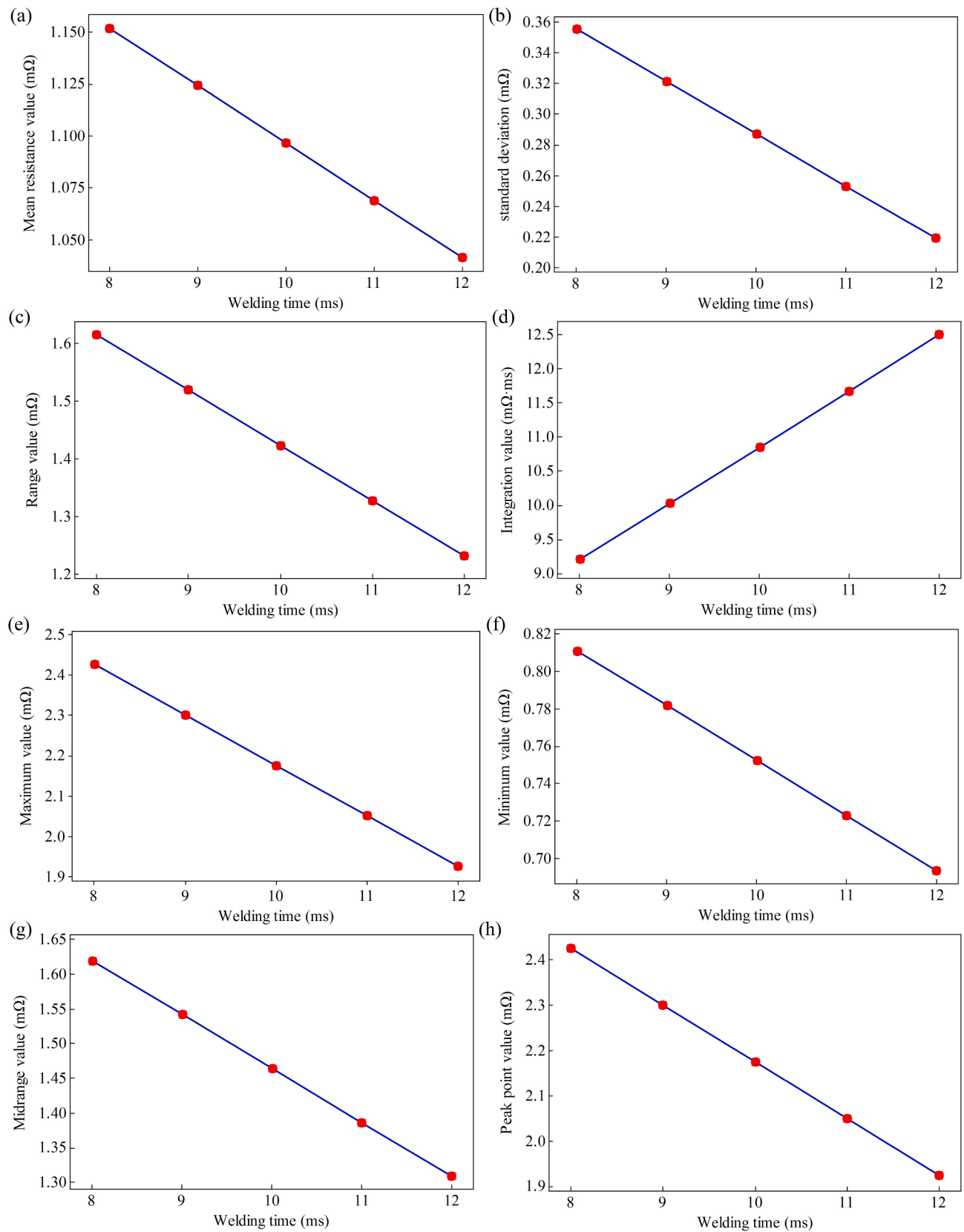


Fig. 16. The effects of the welding time on the mean resistance r_{mean} (a), the standard deviation σ (b), the range Δ (c), the integral value P (d), the maximum value r_{max} (e), the minimum resistance r_{min} (f), the midrange value r_{mid} (g) and the peak resistance r_1 (h).

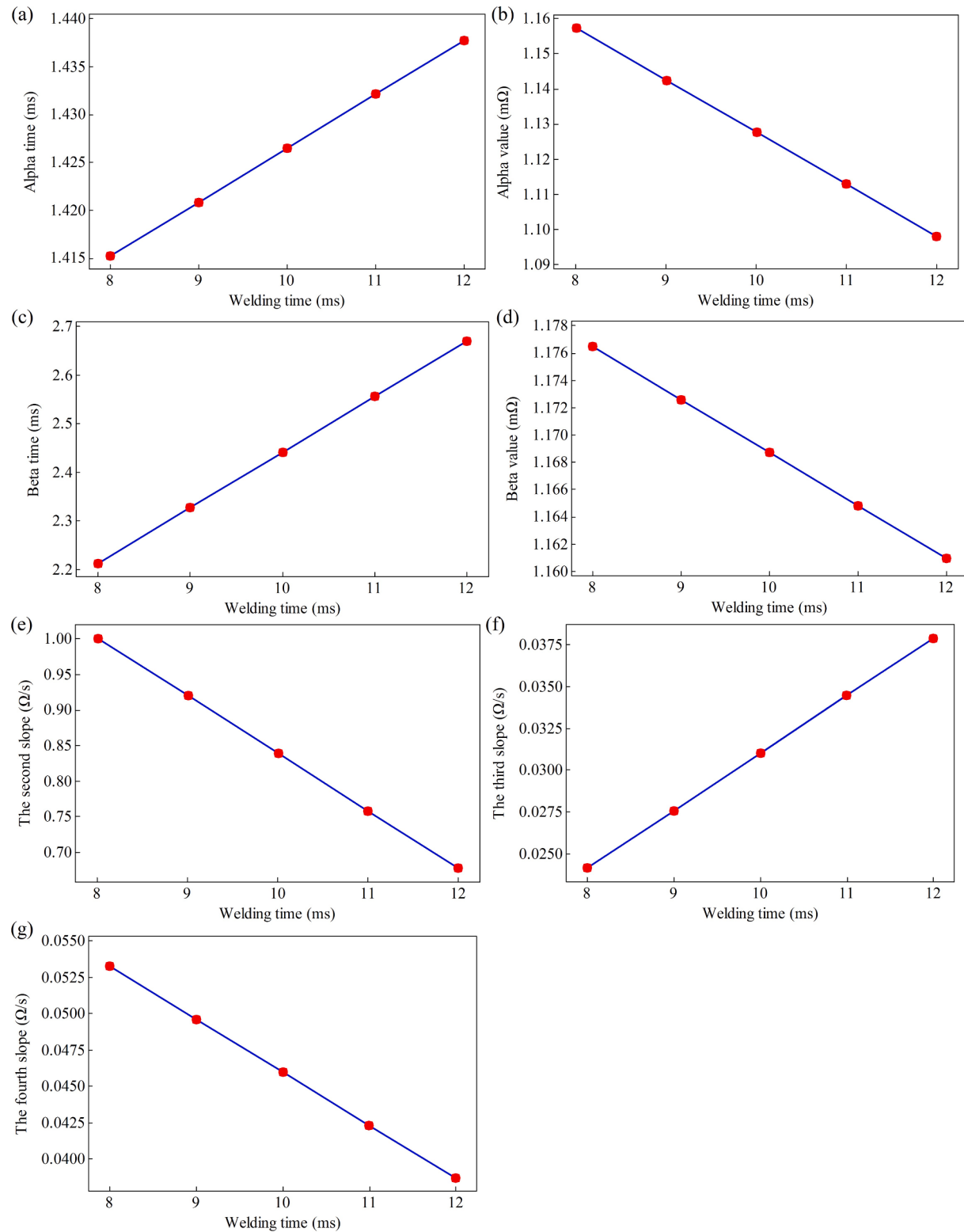


Fig. 17. The effects of the welding time on the alpha time t_α (a), the alpha resistance r_α (b), the beta time t_β (c), the beta resistance r_β (d), the second slope k_2 (e), the third slope k_3 (f) and the fourth slope k_4 (g).

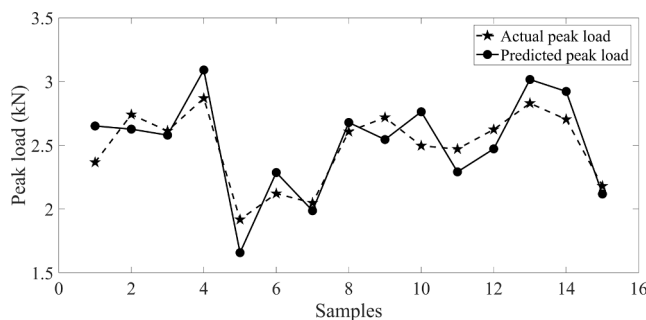


Fig. 18. The accuracy of the regression model.

Table 4

The results of ANOVA for the standard deviation σ .

Source	Sum of squares	df	Mean square	F value	P-value Prob > F
Model	0.1428	4	0.03569	44.5210	0.0053
EP	0.01024	1	0.01024	12.7710	0.0375
WC	0.04234	1	0.04234	52.8117	0.0054
WT	0.03699	1	0.03699	46.1405	0.0065
WC × WT	0.05320	1	0.05320	66.3609	0.0039
Residual	0.002405	3	0.0008017		
Cor Total	0.1452	7			

Notes: standard deviation = 0.02832, mean = 0.2873, R^2 = 0.9834, Adj R^2 = 0.9613, Pred R^2 = 0.8822, PRESS = 0.01710, C. V. % = 9.8572, Adeq precision = 16.9825.

Table 5

The results of ANOVA for the range Δ .

Source	Sum of squares	df	Mean square	F value	P-value Prob > F
Model	3.1355	5	0.6271	283.5113	0.0035
EP	0.3017	1	0.3017	136.4199	0.0073
WC	1.1968	1	1.1968	541.0883	0.0018
WT	0.2959	1	0.2959	133.7985	0.0074
EP × WT	0.1825	1	0.1825	82.5074	0.0119
WC × WT	1.1585	1	1.1585	523.7430	0.0019
Residual	0.004424	2	0.002212		
Cor Total	3.1399	7			

Notes: standard deviation = 0.004424, mean = 1.4236, R^2 = 0.9986, Adj R^2 = 0.9951, Pred R^2 = 0.9775, PRESS = 0.07078, C. V. % = 3.3037, Adeq precision = 39.7987.

Table 6

The results of ANOVA for the resistance at the endpoint r_e .

Source	Sum of squares	df	Mean square	F value	P-value Prob > F
Model	0.5857	1	0.5857	145.7317	< 0.0001
WC	0.5857	1	0.5857	145.7317	< 0.0001
Residual	0.02412	6	0.004019		
Cor Total	0.6099	7			

Notes: standard deviation = 0.06340, mean = 0.8287, R^2 = 0.9605, Adj R^2 = 0.9539, Pred R^2 = 0.9297, PRESS = 0.04287, C. V. % = 7.6506, Adeq precision = 17.0723.

Fig. 13 displays the dynamic resistance signals with different electrode pressures. The effects of different levels of electrode pressures on the features extracted from the dynamic resistance curves are also revealed in Fig. 14. The alpha point and beta point decrease and shift as the electrode pressures become larger. The contact area increases when the electrode pressure increases, at the same time, the length of the conductive pathway also decreases, thus leading to a smaller resistance

Table 7

The results of ANOVA for the numerical integral value P .

Source	Sum of squares	df	Mean square	F value	P-value Prob > F
Model	78.7762	5	15.7552	2371.2047	0.0004
EP	0.1160	1	0.1160	17.4537	0.0528
WC	56.2542	1	56.2542	8466.4083	0.0001
WT	21.5595	1	21.5595	3244.7554	0.0003
EP × WC	0.3646	1	0.3646	54.8691	0.0177
EP × WT	0.4820	1	0.4820	72.5371	0.0135
Residual	0.01329	2	0.006644		
Cor Total	78.7895	7			

Notes: standard deviation = 0.08151, mean = 10.8580, R^2 = 0.9998, Adj R^2 = 0.9994, Pred R^2 = 0.9973, PRESS = 0.2126, C. V. % = 0.7507, Adeq precision = 134.6404.

Table 8

The results of ANOVA for the maximum resistance r_{max} .

Source	Sum of squares	df	Mean square	F value	P-value Prob > F
Model	4.8327	3	1.6109	17.3135	0.0094
WC	3.0778	1	3.0778	33.0792	0.0045
WT	0.5040	1	0.5040	5.4164	0.0805
WC × WT	1.2510	1	1.2510	13.4450	0.0215
Residual	0.3722	4	0.09304		
Cor Total	5.2049	7			

Notes: standard deviation = 0.3050, mean = 2.1758, R^2 = 0.9285, Adj R^2 = 0.8749, Pred R^2 = 0.7140, PRESS = 1.4887, C. V. % = 14.0192, Adeq precision = 9.4182.

Table 9

The results of ANOVA for the minimum resistance r_{min} .

Source	Sum of squares	df	Mean square	F value	P-value Prob > F
Model	0.4636	2	0.2318	36.0704	0.0011
WC	0.4361	1	0.4361	67.8609	0.0004
WT	0.02751	1	0.02751	4.2800	0.0934
Residual	0.03213	5	0.006427		
Cor Total	0.4958	7			

Notes: standard deviation = 0.08017, mean = 0.7522, R^2 = 0.9352, Adj R^2 = 0.9093, Pred R^2 = 0.8341, PRESS = 0.08226, C. V. % = 10.6572, Adeq precision = 11.9010.

Table 10

The results of ANOVA for the midrange value r_{mid} .

Source	Sum of squares	df	Mean square	F value	P-value Prob > F
Model	1.9862	3	0.6621	33.4740	0.0027
WC	1.4578	1	1.4578	73.7033	0.0010
WT	0.1917	1	0.1917	9.6939	0.0358
WC × WT	0.3367	1	0.3367	17.0248	0.0145
Residual	0.07912	4	0.01978		
Cor Total	2.0654	7			

Notes: standard deviation = 0.1406, mean = 1.4640, R^2 = 0.9617, Adj R^2 = 0.9330, Pred R^2 = 0.8468, PRESS = 0.3165, C. V. % = 9.6062, Adeq precision = 12.7112.

value. This is the reason why the mean resistance, standard deviation value, range value, integral value and beta resistance reduce as larger electrode pressure is employed. In this case, the welding heat supplied to the welding zone also decreases as larger electrode pressures are employed. That explains why the alpha time delays with the electrode pressure. To accumulate the same amount of welding heat, more time is needed with higher electrode pressure. As for the increasing rate from

Table 11The results of ANOVA for the median value r_{med} .

Source	Sum of squares	df	Mean square	F value	P-value Prob > F
Model	0.5618	1	0.5618	136.2628	< 0.0001
WC	0.5618	1	0.5618	136.2628	< 0.0001
Residual	0.02474	6	0.004123		
Cor Total	0.5865	7			

Notes: standard deviation = 0.06421, mean = 1.0250, $R^2 = 0.9578$, Adj $R^2 = 0.9508$, Pred $R^2 = 0.9250$, PRESS = 0.04398, C. V. % = 6.2644, Adeq precision = 16.5084.

Table 12The results of ANOVA for the peak location t_1 .

Source	Sum of squares	df	Mean square	F value	P-value Prob > F
Model	0.005854	5	0.001171	2.9544	0.2720
EP	0.00003	1	0.00003	0.07578	0.8089
WC	0.000523	1	0.000523	1.3204	0.3694
WT	0.0000679	1	0.0000679	0.1712	0.7192
EP × WT	0.002045	1	0.002045	5.1598	0.1511
WC × WT	0.003188	1	0.003188	8.0446	0.1051
Residual	0.000793	2	0.000396		
Cor Total	0.006647	7			

Notes: standard deviation = 0.020, mean = 0.25, $R^2 = 0.8808$, Adj $R^2 = 0.5826$, Pred $R^2 = -0.9080$, PRESS = 0.013, C. V. % = 8.09, Adeq precision = 4.884.

Table 13The results of ANOVA for the peak resistance r_1 .

Source	Sum of squares	df	Mean square	F value	P-value Prob > F
Model	4.8346	3	1.6115	17.3246	0.0093
WC	3.0789	1	3.0789	33.0998	0.0045
WT	0.5035	1	0.5035	5.4129	0.0806
WC × WT	1.2522	1	1.2522	13.4612	0.0214
Residual	0.3721	4	0.09302		
Cor Total	5.2067	7			

Notes: standard deviation = 0.3050, mean = 2.1756, $R^2 = 0.9285$, Adj $R^2 = 0.8749$, Pred $R^2 = 0.7142$, PRESS = 1.4883, C. V. % = 14.0185, Adeq precision = 9.4222.

Table 14The results of ANOVA for the alpha time t_α .

Source	Sum of squares	df	Mean square	F value	P-value Prob > F
Model	0.1497	5	0.02994	29.2350	0.0334
EP	0.02122	1	0.02122	20.7156	0.0450
WC	0.08778	1	0.08778	85.7022	0.0115
WT	0.001013	1	0.001013	0.9885	0.4249
EP × WC	0.009941	1	0.009941	9.7052	0.0894
WC × WT	0.02977	1	0.02977	29.0632	0.0327
Residual	0.002049	2	0.001024		
Cor Total	0.1518	7			

Notes: standard deviation = 0.032, mean = 1.4265, $R^2 = 0.9865$, Adj $R^2 = 0.9527$, Pred $R^2 = 0.7840$, PRESS = 0.03278, C. V. % = 2.2435, Adeq precision = 15.6768.

the alpha point and beta point, although the resistance value declines as the electrode pressures go up, the time reaching these key points also changes, the slope increases instead of decreasing.

Three dynamic resistance signals with different welding times are presented in Fig. 15. Different levels of the extracted features which are plotted according to the models (4)-(22) are also exhibited in Fig. 16 and Fig. 17. The mean resistance, standard deviation, range value, maximum value, minimum value, midrange value, peak resistance, alpha

Table 15The results of ANOVA for the alpha resistance r_α .

Source	Sum of squares	df	Mean square	F value	P-value Prob > F
Model	0.2040	3	0.06801	43.5580	0.0016
WC	0.1789	1	0.1789	114.5597	0.0004
WT	0.007033	1	0.007033	4.5046	0.1011
WC × WT	0.01813	1	0.01813	11.6096	0.0271
Residual	0.006245	4	0.001561		
Cor Total	0.2103	7			

Notes: standard deviation = 0.03951, mean = 1.1277, $R^2 = 0.9703$, Adj $R^2 = 0.9480$, Pred $R^2 = 0.8812$, PRESS = 0.02498, C. V. % = 3.5038, Adeq precision = 14.1106.

Table 16The results of ANOVA for the beta time t_β .

Source	Sum of squares	df	Mean square	F value	P-value Prob > F
Model	5.4220	2	2.7110	49.1701	0.0005
WC	5.0039	1	5.0039	90.7561	0.0002
WT	0.4182	1	0.4182	7.5842	0.0401
Residual	0.2757	5	0.05514		
Cor Total	5.6977	7			

Notes: standard deviation = 0.2348, mean = 2.4416, $R^2 = 0.9516$, Adj $R^2 = 0.9322$, Pred $R^2 = 0.8761$, PRESS = 0.7057, C. V. % = 9.6169, Adeq precision = 14.1803.

Table 17The results of ANOVA for the beta resistance r_β .

Source	Sum of squares	df	Mean square	F value	P-value Prob > F
Model	0.2742	6	0.04570	3806.9586	0.0124
EP	0.0002904	1	0.0002904	24.1903	0.1277
WC	0.2591	1	0.2591	21585.0067	0.0043
WT	0.0004836	1	0.0004836	40.2836	0.0995
EP × WC	0.004131	1	0.004131	344.1403	0.0343
EP × WT	0.004990	1	0.004990	415.6606	0.0312
WC × WT	0.005192	1	0.005192	432.4702	0.0306
Residual	0.00001201	1	0.00001201		
Cor Total	0.2742	7			

Notes: standard deviation = 0.003465, mean = 1.1688, $R^2 = 0.9999$, Adj $R^2 = 0.9996$, Pred $R^2 = 0.9972$, PRESS = 0.000768, C. V. % = 0.2964, Adeq precision = 140.8033.

Table 18The results of ANOVA for the initial resistance r_0 .

Source	Sum of squares	df	Mean square	F value	P-value Prob > F
Model	1.2230	1	1.2230	3.9831	0.0930
WC	1.2230	1	1.2230	3.9831	0.0930
Residual	1.8422	6	0.3070		
Cor Total	3.0652	7			

Notes: standard deviation = 0.5541, mean = 0.9546, $R^2 = 0.3990$, Adj $R^2 = 0.2988$, Pred $R^2 = -0.06847$, PRESS = 3.2751, C. V. % = 58.0488, Adeq precision = 2.8224.

resistance and beta resistance decrease with the welding time. The function of welding time is accumulating welding heat for the welding nugget growth. According to Fig. 15, the first two stages of the dynamic resistance seem to be quite different from others. Dynamic resistance with longer welding time is more gentle, while its integration value is larger than those with shorter welding times. Since the integration value

Table 19The results of ANOVA for the first slope k_1 .

Source	Sum of squares	df	Mean square	F value	P-value Prob > F
Model	54.3494	5	10.8699	1.9848	0.3681
EP	0.0370	1	0.0370	0.006763	0.9419
WC	9.0919	1	9.0919	1.6601	0.3265
WT	0.0281	1	0.0281	0.005136	0.9494
EP × WT	27.1882	1	27.1882	4.9644	0.1557
WC × WT	18.0042	1	18.0042	3.2875	0.2115
Residual	10.9532	2	5.4766		
Cor Total	65.3026	7			

Notes: standard deviation = 2.3402, mean = 5.2548, R^2 = 0.8323, Adj R^2 = 0.4129, Pred R^2 = -1.6837, PRESS = 175.2515, C. V. % = 44.5351, Adeq precision = 4.2845.

Table 20The results of ANOVA for the second slope k_2 .

Source	Sum of squares	df	Mean square	F value	P-value Prob > F
Model	1.3893	3	0.4631	11.4936	0.0195
WC	0.7887	1	0.7887	19.5747	0.0115
WT	0.2091	1	0.2091	5.1906	0.0849
WC × WT	0.3915	1	0.3915	9.7154	0.0356
Residual	0.1612	4	0.04029		
Cor Total	1.5505	7			

Notes: standard deviation = 0.2007, mean = 0.8393, R^2 = 0.8961, Adj R^2 = 0.8181, Pred R^2 = 0.5842, PRESS = 0.6447, C. V. % = 23.9168, Adeq precision = 7.5413.

is directly proportional to the welding time, longer welding time indicates a larger integral value. The locations and values of several key points are different, so the slopes between them have also changed with different welding time values.

Table 23 lists the correlation coefficient matrix between the exacted features and the mechanical properties of the welding joints. According to the results, the features mean resistance r_{mean} , the value of the endpoint r_e , the median value r_{med} , the alpha resistance r_α , and the beta resistance r_β are closely related to the peak load F , the maximum displacement L , and the failure energy Q . These five features are also highly affected by the welding process parameters. Since the welding process parameters are the basic parameters generating the welding joints with different welding qualities. In addition, 68 groups of the features were extracted from the dynamic resistance signal. The five features were used to express the variations of the dynamic resistance and predict the peak load of the welded joints. 53 welding joints were chosen at random to develop the regression model, while the remaining 15 groups were utilized to test the accuracy of the model. The mathematical model quantifying the relationship between the extracted features and the welding quality was established based on the stepwise

Table 21The results of ANOVA for the third slope k_3 .

Source	Sum of squares	df	Mean square	F value	P-value Prob > F
Model	0.0003147	5	0.000629	21.8908	0.0443
EP	0.000818	1	0.000818	28.4557	0.0334
WC	0.000411	1	0.000411	14.2912	0.0634
WT	0.000378	1	0.000378	13.1571	0.0683
EP × WC	0.000683	1	0.000683	23.7428	0.0396
WC × WT	0.000857	1	0.000857	29.8069	0.0320
Residual	0.0000575	2	0.0000288		
Cor Total	0.003204	7			

Notes: standard deviation = 0.005362, mean = 0.03103, R^2 = 0.9821, Adj R^2 = 0.9372, Pred R^2 = 0.7129, PRESS = 0.00092, C. V. % = 17.2800, Adeq precision = 11.8999.

Table 22The results of ANOVA for the fourth slope k_4 .

Source	Sum of squares	df	Mean square	F value	P-value Prob > F
Model	0.000902	2	0.000451	8.1789	0.0265
WC	0.000475	1	0.000475	8.6076	0.0325
WT	0.000427	1	0.000427	7.7503	0.0387
Residual	0.000276	5	0.0000551		
Cor Total	0.001178	7			

Notes: standard deviation = 0.007426, mean = 0.046, R^2 = 0.7659, Adj R^2 = 0.6723, Pred R^2 = 0.4007, PRESS = 0.00071, C. V. % = 16.1433, Adeq precision = 6.6024.

Table 24

ANOVA results of the regression model.

Source	Sum of squares	df	Mean square	F value	P-value Prob > F
Model	26.1641	4	6.5410	83.7324	<0.0001
Residual	3.7497	48	0.0781		
Cor total	29.9137	52	0.5753		
Standard deviation	0.2795	Mean	2.1593		
R-Squared	0.8747	Adjusted R-Squared	0.8642		

regression method. The significance of each term in the quadratic polynomial function was checked by its P-value. If its P-value is larger than 0.1, this term should be rejected. The results of the ANOVA are shown in **Table 24** and **Table 25**. The terms of r_e , $r_{mean} \times r_\beta$, $r_e \times r_\beta$ and $r_{med} \times r_\alpha$ have been retained since their P-values are less than 0.1. The model is also quite significant. The adjusted R^2 is quite close to the determination R^2 . Generally speaking, the results signify that the developed model is sufficient to navigate its design space. The regression coefficients for the model were calculated and presented as follows,

Table 23

The correlation coefficients between the extracted features and the mechanical performances of the welded joints.

	r_{mean} mΩ	σ mΩ	Δ mΩ	r_e mΩ	P mΩ·ms	r_{max} mΩ	r_{min} mΩ	r_{mid} mΩ	r_{med} mΩ
F (kN)	0.98	0.69	0.73	0.98	0.69	0.85	0.92	0.90	0.97
L (mm)	0.72	0.62	0.63	0.69	0.29	0.69	0.66	0.71	0.70
Q (J)	0.90	0.66	0.70	0.89	0.54	0.80	0.85	0.84	0.89
	r_1 mΩ	t_α ms	r_α mΩ	t_β ms	r_β mΩ	k_2 Ω/s	k_3 Ω/s	k_4 Ω/s	
F (kN)	0.85	0.79	0.95	0.83	0.95	0.81	0.18	0.52	
L (mm)	0.69	0.42	0.71	0.49	0.68	0.70	0.08	0.01	
Q (J)	0.80	0.57	0.88	0.71	0.88	0.79	0.24	0.26	

Table 25
ANOVA results of each item in the regression model.

Term	Estimated value	Standard error	T value	P-value
Constant term	5.9414	0.3505	16.9521	<0.0001
r_e	-7.1453	0.8142	-8.7762	<0.0001
$r_{mean} \times r_\beta$	-2.4898	0.7579	-3.2852	0.0019
$r_e \times r_\beta$	3.5581	0.7400	4.8079	<0.0001
$r_{med} \times r_a$	1.6137	0.6301	2.5612	0.0136

Table 26
Statistical parameters of the performances of the developed regression model.

Statistical parameters	Equations	Value
Δ	$\Delta = \max F_{i,pre} - F_{i,exp} $	0.2847 kN
RSME	$RSME = \sqrt{\frac{\sum_{i=1}^n (F_{i,pre} - F_{i,exp})^2}{n}}$	0.1808
MAE	$MAE = \frac{\sum_{i=1}^n F_{i,pre} - F_{i,exp} }{n}$	0.1633
MSE	$MSE = \frac{\sum_{i=1}^n (F_{i,pre} - F_{i,exp})^2}{n}$	0.0327
MAPE	$MAPE = \frac{1}{n} \sum_{i=1}^n \left \frac{F_{i,pre} - F_{i,exp}}{F_{i,exp}} \right \times 100\%$	6.66%
EC	$EC = 1 - \frac{\sqrt{\sum_{i=1}^n (F_{i,pre} - F_{i,exp})^2}}{\sqrt{\sum_{i=1}^n F_{i,pre}^2} + \sqrt{\sum_{i=1}^n F_{i,exp}^2}}$	96.41%

Notes: root mean square error (RMSE), mean absolute error (MAE), mean square error (MSE), mean absolute percentage error (MAPE), equality coefficient (EC).

$$F = 5.9414 - 7.1453 \times r_e - 2.4898 \times r_{mean} \times r_\beta + 3.5581 \times r_e \times r_\beta + 1.6137 \times r_{med} \times r_a \quad (23)$$

Fig. 18 presents the accuracy of the welding quality prediction model, while the statistical parameters of the performances of this model are shown in Table 26. The maximum relative error of this model is less than 10%, which indicates the regression model utilizing the extracted features presents quite good performance for welding quality assessment and prediction. Therefore, it should be concluded that these five extracted features can be treated as the most significant features which can present both the dynamic resistance signal and the welding quality. Using these features can effectively monitor and evaluate the welding quality.

4. Conclusions

- (1) Twenty features were extracted from the dynamic resistance signal to express its information and variations. The results of ANOVA demonstrate that the features t_1 , r_0 and k_1 are not sensitive to the changes in the welding process parameters.
- (2) The welding current is the most significant factor for all the extracted factors except for σ and k_3 according to its P-value. The electrode pressure is quite related to only seven extracted features and it is the least significant parameter among the three welding parameters (welding current, welding time and electrode pressure) except for the features Δ and k_3 . The features r_e and r_{med} are only influenced by the welding current.
- (3) The feature r_{mean} ranks first regarding the effect degree of the extracted five features and it affects the peak load of the welded joints by its straight effect; while the features r_e , r_{med} , r_a and r_β influence the welding quality through the interaction effects.
- (4) The developed model quantifying the relationship between the extracted features and peak load of the welded joints can predict and assess the welding quality with sound performances. The maximum relative error is less than 10%.

- (5) The features selected from the dynamic resistance signal to predict the welding quality are the ones with extremely high Pred R^2 values. All the Pred R^2 values of the regression models quantifying the relationships between these features and welding process parameters are above 0.9. It implies that the features highly related to the process parameters may need to be selected when controlling welding quality.

CRediT authorship contribution statement

Dawei Zhao: Conceptualization, Methodology, Writing - review & editing, Visualization. **Yuriy Bezgans:** Software, Resources, Data curation. **Yuanxun Wang:** Supervision, Investigation. **Wenhai Du:** Software, Validation, Investigation. **Nikita Vdonin:** Writing - original draft, Formal analysis.

Declaration of Competing Interest

The authors declare that they have no known competing financial interests or personal relationships that could have appeared to influence the work reported in this paper.

Acknowledgments

The authors are grateful for the financial support provided by the Natural Science Foundation of Shandong Province (ZR2016EEM47/ZR2018PEE004) and open projects of State Key Laboratory for Strength and Vibration of Mechanical Structures (SV2019-KF-39). The authors are also grateful for the support for conducting our experiment provided by the analysis and test center of Huazhong University of Science and Technology and Dongfeng Peugeot Citroen Automobile Company Limited.

Appendix

See Tables 4–22.

References

- [1] A. Ghosh, S. Chattopadhyaya, N.K. Singh, Prediction of weld bead parameters, transient temperature distribution & HAZ width of submerged arc welded structural steel plates, Defect Diffus. Forum 326 (2012) 405–409.
- [2] C. Summerville, P. Compston, M. Doolan, A comparison of resistance spot weld quality assessment techniques, Proc. Manuf. 29 (2019) 305–312.
- [3] A. Taram, C. Roquelet, P. Meilland, T. Dupuy, C. Kaczynski, J.L. Bodnar, T. Duvaut, Nondestructive testing of resistance spot welds using eddy current thermography, Appl. Opt. 57 (2018) D63–D68.
- [4] B. Xing, Y. Xiao, Q.H. Qin, Characteristics of shunting effect in resistance spot welding in mild steel based on electrode displacement, Measurement 115 (2018) 233–242.
- [5] D.W. Dickinson, J.E. Franklin, A. Stanya, Characterization of spot welding behavior by dynamic electrical parameter monitoring, Weld. J. 59 (1980) 170s–176s.
- [6] S.A. Gedeon, C.D. Sorensen, K.T. Ulrich, T.W. Eagar, Measurement of dynamic electrical and mechanical properties of resistance spot welds, Weld. J. 66 (1987) 378–385.
- [7] C. Ma, S.D. Bhole, D.L. Chen, A. Lee, E. Biro, G. Boudreau, Expulsion monitoring in spot welded advanced high strength automotive steels, Sci. Technol. Weld. Joining 11 (2006) 480–487.
- [8] Y. Cho, S. Rhee, Primary circuit dynamic resistance monitoring and its application to quality estimation during resistance spot welding, Weld. J. 81 (2002) 104s–111s.
- [9] Y.C. Chen, K.H. Tseng, Y.S. Cheng, Electrode displacement and dynamic resistance during small-scale resistance spot welding, Adv. Sci. Lett. 11 (2012) 72–79.
- [10] K.K. Karama, B.W. Ikua, G.N. Nyakoe, A.A. Abdallah, K. Mombasa, Development of an intelligent on-line monitoring system based on ANFIS algorithm for resistance spot welding process, J. Inform. Eng. Appl. 5 (2015) 33–39.
- [11] S.W. Shin, J.H. Lee, S.H. Park, A study on the prediction of nugget diameter of resistance spot welded part of 1.2 GPa ultra high strength TRIP steel for vehicle, J. Korea Acad.-Indu. Cooperat. Soc. 19 (2018) 52–60.
- [12] S.W. Shin, J.H. Lee, S.H. Park, Strength estimation model of resistance spot welding of 1.2 GPa grade ultra high strength TRIP steel for car body applications, J. Welding Joining 36 (2018) 82–89.

- [13] B. Xing, Y. Xiao, Q.H. Qin, H. Cui, Quality assessment of resistance spot welding process based on dynamic resistance signal and random forest based, *Int. J. Adv. Manuf. Technol.* 94 (2018) 327–339.
- [14] H. Sun, J. Yang, L. Wang, Resistance spot welding quality identification with particle swarm optimization and a kernel extreme learning machine model, *Int. J. Adv. Manuf. Technol.* 91 (2017) 1879–1887.
- [15] L. Wang, Y. Hou, H. Zhang, J. Zhao, T. Xi, X. Qi, Y. Li, A new measurement method for the dynamic resistance signal during the resistance spot welding process, *Meas. Sci. Technol.* 27 (2016) 1–12.
- [16] M.F.A. Zaharuddin, D. Kim, S. Rhee, An ANFIS based approach for predicting the weld strength of resistance spot welding in artificial intelligence development, *J. Mech. Sci. Technol.* 31 (2017) 5467–5476.
- [17] Y. Luo, R. Wan, Z. Yang, X. Xie, Study on the thermo-effect of nugget growing in single-phase AC resistance spot welding based on the calculation of dynamic resistance, *Measurement* 78 (2016) 18–28.
- [18] J. Wen, H.D. Jia, C.S. Wang, Quality estimation system for resistance spot welding of stainless steel, *ISIJ Int.* 59 (2019) 2073–2076.
- [19] H. Zhang, Y. Hou, T. Yang, Q. Zhang, J. Zhao, Welding quality evaluation of resistance spot welding using the time-varying inductive reactance signal, *Meas. Sci. Technol.* 29 (2018), 055601.
- [20] Q. Fan, G. Xu, X. Gu, Expulsion characterization of stainless steel resistance spot welding based on dynamic resistance signal, *J. Mater. Process. Technol.* 236 (2016) 235–240.
- [21] Y.J. Xia, Z.W. Su, Y.B. Li, L. Zhou, Y. Shen, Online quantitative evaluation of expulsion in resistance spot welding, *J. Manuf. Processes* 46 (2019) 34–43.
- [22] D.K. Gope, U. Kumar, S. Chattopadhyaya, S. Mandal, Experimental investigation of pug cutter embedded TIG welding of Ti-6Al-4V titanium alloy, *J. Mech. Sci. Technol.* 32 (2018) 2715–2721.
- [23] W. Tan, Y. Zhou, H.W. Kerr, S. Lawson, A study of dynamic resistance during small scale resistance spot welding of thin Ni sheets, *J. Phys. D Appl. Phys.* 37 (2004) 1998–2008.
- [24] Y.R. Wong, X. Pang, A new characterization approach of weld nugget growth by real-time input electrical impedance, *Engineering* 6 (2014) 516–525.
- [25] E.A. Bel'skaya, E.Y. Kulyamina, Electrical resistivity of titanium in the temperature range from 290 to 1800 K, *High Temperat.* 45 (2007) 785–796.
- [26] D. Zhao, Y. Wang, D. Liang, M. Ivanov, Performances of regression model and artificial neural network in monitoring welding quality based on power signal, *J. Mater. Res. Technol.* 9 (2020) 1231–1240.
- [27] K. Zhong, Q. Wang, Optimization of ultrasonic extraction of polysaccharides from dried longan pulp using response surface methodology, *Carbohydr. Polym.* 25 (2010) 19–25.
- [28] K.I. Yaakob, M. Ishak, M.M. Quazi, M.N.M. Salleh, Optimizing the pulse wave mode low power fibre laser welding parameters of 22MnB5 boron steel using response surface methodology, *Measurement* 135 (2019) 452–466.